atmosphere

MDPI

Article

Influence of Relative Humidity on the Characteristics of Filter Cake Using Particle Flow Code Simulation

Dinglian Shi, Jianlong Li *, Yongnan Du, Quanquan Wu *, Shan Huang, Hong Huang and Daishe Wu

School of Resources & Environment, Nanchang University, Nanchang 330031, China; dlshi@email.ncu.edu.cn (D.S.); duyongnan@email.ncu.edu.cn (Y.D.); coral119@ncu.edu.cn (S.H.); honghuang@ncu.edu.cn (H.H.); dswu@ncu.edu.cn (D.W.)
* Correspondence: jlli@ncu.edu.cn (J.L.); quanquanwu@email.ncu.edu.cn (Q.W.)

Abstract: To study the effect of air humidity on particle filtration performance, the Particle Flow Code (PFC) calculation program was used to numerically simulate the formation process of filter cake. The effects of relative air humidity on the deposition morphology, porosity and filtration resistance characteristics of the filter cake were revealed. The results show that relative humidity (RH) is mainly reflected in the density and surface viscosity of the particles. It was found that the higher the relative humidity, the higher the particle moisture content, the greater the density, and the greater the surface viscosity. With an increase in the particle density or with a decrease in the viscosity, the bridging phenomenon of particle deposition became more obvious; the dendritic deposition phenomenon became weaker; and, therefore, the filter cake structure became denser; the porosity decreased; and the total filtration resistance increased. As the humidity changed, the actual density and viscosity of the particles changed simultaneously with different degrees, which caused different variation trends of the filter cake characteristics. Three different types of particles, DM828 (Starch), PVA1788 (Polyvinyl Alcohol) and Polyacrylamide (Polyacrylic acid), were selected for comparison. For the studied PVA1788 and Polyacrylamide particles, with an increase in relative humidity, the porosity of the filter cake increased monotonously, while the total filtration resistance decreased monotonously. For DM828 particles, the cake porosity first decreased and then increased, and the total filtration resistance first increased and then decreased, with an inflection point at 30% RH. By combining these results with existing reports, three kinds of variations of the filtration performance with humidity could be determined: (1) as the humidity increased, the filtration resistance first increased and then decreased; (2) the filtration resistance decreased; and (3) the filtration resistance increased.

Keywords: filter cake; relative humidity; numerical simulation; porosity; filtration resistance; rolling resistance model

check for updates

Citation: Shi, D.; Li, J.; Du, Y.; Wu, Q.; Huang, S.; Huang, H.; Wu, D. Influence of Relative Humidity on the Characteristics of Filter Cake Using Particle Flow Code Simulation. *Atmosphere* **2022**, *13*, 770. https://doi.org/10.3390/atmos13050770

Academic Editor: Chuen-Jinn Tsai

Received: 28 March 2022
Accepted: 9 May 2022
Published: 10 May 2022

Publisher's Note: MDPI stays neutral with regard to jurisdictional claims in published maps and institutional affiliations.

Copyright: © 2022 by the authors. Licensee MDPI, Basel, Switzerland. This article is an open access article distributed under the terms and conditions of the Creative Commons Attribution (CC BY) license (https://creativecommons.org/licenses/by/4.0/).

1. Introduction

The environment, food, chemical industry, mining, machining, painting, metallurgy and other industries generate a large number of particulates [1–3]. Particulate matters can persist for a long time, migrate and spread widely, and they pose significant risks to human health and the environment [4]. Long-term exposure to air pollution particles may induce occupational diseases. It can cause or aggravate cardiovascular and respiratory diseases [5–7]. It also significantly affects air quality in cities [8,9].

Filtration technology can capture fine particles efficiently, and it is widely used in industry [10–14]. For some industrial workplaces where the environment is humid, the moisture absorption of the particles can significantly affect the performance of the filtration system [15,16]. The air humidity can increase the moisture content of the particles and increase the liquid bridge force in particle–particle and particle–filter medium contact. The corresponding macroscopic performance is an increase in the particle viscosity, which significantly affects the filter cake structure and directly affects the filtration resistance. Filtration resistance, as an important indicator for the evaluation of filtration performance,

is related to the energy consumption and efficiency of filtration equipment. Furthermore, as a key parameter of the filter cake structure, porosity plays an important role in the filtration resistance. The resistance is inversely proportional to the square of the filter cake porosity [17]. In the industrial production process, it is particularly required to improve the filtration efficiency and reduce the filtration resistance when the humidity conditions are high.

Qing et al. [18] analyzed the contribution of the interaction force between particles to the adhesion force under different relative humidity conditions by using a self-made device to test the micro-friction force and adhesion force, and they concluded that the adhesion force increased with an increase in relative humidity. Xue et al. [19] studied the surface deposition characteristics of viscous particles on the filter material in a high-humidity environment, introduced the liquid bridge force model and calculated the force of the particles, and they found that the error between the particle force and the liquid bridge force model was within 6%. The relative humidity of the environment affected the liquid bridge volume between particles, and the contact force affected the particle deposition. Zhan [20] established a numerical model under two conditions of drying and moisture absorption, and analyzed the particle movement trajectory and particle distribution characteristics when the surface of the heat exchanger was dry and wet, and they revealed that an increase in relative air humidity can generate more condensed droplets on the fin surface, significantly increase the deposition of wet particles and increase the pressure drop. Gupta et al. [21] studied the effects of humidity and particle hygroscopicity on the mass carrying capacity of High Efficiency Particulate Air (HEPA) filters, and it was found that the specific cake resistance, which was computed for different test conditions and used as a measure of the mass loading capacity, decreased with an increase in humidity for non-hygroscopic aluminum oxide particles and for hygroscopic NaCl particles (at humidities below the deliquescent point). Ribeyre et al. [22] investigated the impact of relative humidity changes on the pressure drop of a nanostructured deposit, and the results showed that, for three different non-hygroscopic nanostructured cakes, the pressure drop of the deposit increased when the relative humidity increased, while the bed thickness decreased. Li et al. [23] applied the Particle Flow Code to dynamically simulate the deposition form of viscous particles on the surface of the filter material, and they obtained the corresponding relationships between the rolling resistance coefficient, friction coefficient, porosity and filtration resistance of different viscous particles. Boudhan et al. [24] studied the influence of air humidity on particle filtration performance of a pulse-jet bag filter, and their experimental results showed that the air humidity may significantly increase the particulate cake resistance to airflow because of water capillary condensation leading to the formation of compact particulate cake. The studies carried out by Joubert et al. [25,26], Li et al. [15] and Yuan et al. [27] found that the filtration resistance decreased with an increase in humidity. Li et al. [28] found that particles with different moisture contents formed cakes, with the filtration resistance first increasing and then decreasing with an increase in humidity.

Existing research has made a lot of beneficial progress on the effect of particle viscosity on deposition. Different kinds of variations of cake porosity and filtration resistance with humidity have been revealed in the literature. However, simulations of the filter cake structure often focus on a single characteristic of the particle, and the differentiation in the changes of multiple particle parameters changing simultaneously with the moisture absorption quantity are not considered enough. There is a scarcity of research on simultaneous changes in surface viscosity and the density of actual particles after hygroscopic equilibrium.

In this paper, based on the PFC calculation program, the influence of particle filtration performance is studied, and the influence of environmental humidity on the deposition morphology, porosity and filtration resistance characteristics of filter cake is revealed. The influences of parameters such as particle density and the rolling resistance coefficient on particle deposition behavior are discussed. The research conclusions are helpful in providing a better understanding of the mechanism of influence of particle viscosity in the filtration system and in finding solutions for high-efficiency filtration in a humid environment.

2. Materials and Methods

PFC software is based on the particle flow discrete element method, which can simulate the movement of particles under specific force conditions and the interaction between particles, and then analyze the mechanical properties between particles. Throughout the entire simulation process, PFC software treats particle flow media as a series of discrete, independently moving particles.

The contact models of particle flow include the linear model, stiffness model, sliding model, bonding model, rolling resistance model etc. [29]. This paper selects the rolling resistance model (rrlinear); this model is based on the linear model and adds a rolling resistance mechanism, which is reflected in the ball–ball and ball–surface contact. The rolling resistance model is based on the addition of contact torque to hinder the rolling process of particles, which can more realistically reflect the particle deposition. The linear rolling resistance contact model behaves similarly to the linear model, except that the internal moment increases linearly with the accumulated relative rotation of the contacts at the point of contact. The maximum value of this accumulation is equal to the current normal force multiplied by the coefficient of rolling resistance and the effective contact radius [30]. The constant that relates the increase in internal moment to the relative rotational increase at the point of contact is expressed as rolling stiffness.

The rolling resistance stiffness (k_r) is defined as

$$k_r = k_s \overline{R}^2 \tag{1}$$

where k_s is the shear stiffness, and $\overline{R}^2$ is the contact effective radius.

The calculation of the contact force and moment in the rolling resistance model is shown in Equation (2):

$$F_c = F^d + F^l, \; M_c = M^r \tag{2}$$

where F_c is the contact force, F^d is the dashpot force, F^l is the linear force, M_c is the contact resistance moment, and M^r is the rolling resistance moment.

The particles on the filter material are mainly affected by the van der Waals force, the solid bridge force, the liquid bridge force, the electrostatic force and other adhesion forces. In an environment with high humidity, the van der Waals force and liquid bridge force dominate the adhesion force [31], and the electrostatic force is easy to release, the influence of which can be ignored. The critical relative humidity for the disappearance of the liquid bridge force is between 60% and 80% [22,32,33]. Thus, the upper relative humidity is considered to be 80% in this study. The increase in the adhesion between the particles will lead to an increase in the coefficient of rolling resistance and the coefficient of friction between the filter cake particles. The influence of the friction coefficient is much weaker than that of the rolling resistance coefficient [23,34], so this paper only considers the influence of the rolling resistance coefficient.

The model is 2D, and the following simplifications and assumptions are given: (a) in the process of particle filtration, the filtration velocity is constant and uniformly distributed; (b) no rebound occurs when a particle comes into contact with other particles or the wall; (c) the particles will not pass through the filter cake or filter medium; and (d) the rolling resistance coefficient of the particles is linearly positively related to the adhesion.

By establishing the corresponding relationship between the particle density and the rolling resistance coefficient with the relative humidity, the simulation of particle deposition under varying environmental humidities can be carried out. The values of the particle mesoscopic parameters in the model [35–38] are shown in Table 1.

The filtration resistance of the filter cake is analyzed by dividing it into layers, and the value of the layer height in this paper is six times the diameter of the particles. Then, the Carman–Kozeny Equation [39] is used to calculate the filtration resistance of the filter cake:

$$\Delta P_i = K_0 \left(\frac{6}{d_p} \right)^2 \frac{(1-\varepsilon_i)^2}{\varepsilon_i^3} V_s \mu d_p \tag{3}$$

where ΔP_i is the filtration resistance of the i-th layer; K_0 is the Karman constant; d_p is the particle diameter; V_s is the filtration wind speed; μ is the fluid viscosity; and ε_i is the porosity of the i-th layer, $\varepsilon_i = \frac{6L - \pi d_p n_i}{6L}$, where n_i is the number of particles contained in the i-th layer in the particle layer, and L is the length of the filter material.

The total filtration resistance is calculated as follows:

$$\Delta P_t = \sum_{i=1}^{n} \Delta P_i \quad (4)$$

where ΔP_t is the total filtration resistance, and n is the number of particle layers.

Table 1. Values of main parameters of particles in the model.

Items	Values
Elastic modulus (E_c, Pa)	1.0×10^8
Stiffness ratio (k_n/k_s, -)	2.0
Friction coefficient (β, -)	1.5
Rolling resistance coefficient (α, -)	0.0–1.0
Particle radius (r_p, μm)	5
Particle density (ρ, kg· m^{-3})	500–3000
Number of particles (n, -)	2000

3. Results and Discussion

3.1. Deposition Morphology of Particles

The simulated particle deposition process with a density of 1000 kg/m^3 and a rolling resistance coefficient of 0.5 is shown in Figure 1. A computer with a CPU model of i7-10870H, a main frequency of 2.2 GHz and a RAM of 12 G was used for calculation, and the calculation time was about 20 min for each case. Initially, the particles were randomly distributed in the computational domain. During the deposition process of the particles on the surface of the filter material, the movement form included not only the sliding on the surface of the existing deposited particles but also the rolling of the particles themselves so that the particles were gradually deposited by the "bridging" (e.g., most of the particles in regions A1 and A2) or "dendritic" phenomenon (e.g., most of the particles in regions B1 and B2). The "bridging" phenomenon describes the situation in which the particles slide down on the deposited particles, connecting more with adjacent particles, making the particle layer more compact. A "dendritic" structure occurs when the particles are sticky enough to resist slipping, so they stick to the particles that have already been deposited and no longer roll down, resulting in a more stable and looser structure. From 15 to 20 min, the particles moved (sliding or rolling) relatively slowly and tended to stably deposit. Finally, the particle deposition morphology became stable, and there was a certain porosity.

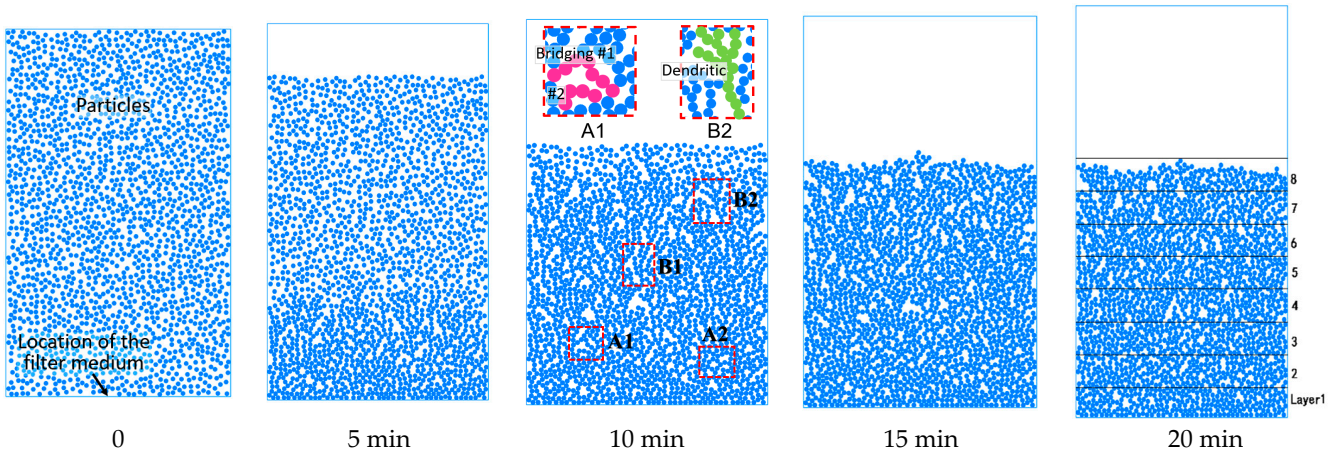


Figure 1. The deposition process of particles on the surface of the filter medium.

Figure 2 shows the particle deposition morphologies under conditions of a density of 1000 or 2500 kg/m^3 and a rolling resistance coefficient of 0.2 or 0.5. Comparing Figure 2a,b, it was found that the greater the density, the more obvious that the "bridging" phenomenon occurred in the filter cake. The deposition morphology corresponding to a density of 2500 kg/m^3 (Figure 2b) was tighter than that of 1000 kg/m^3 (Figure 2a). This was mainly because the adhesion force between particles was not enough to counteract the downward movement trend caused by the particle's gravity. Comparing Figure 2a,c, the particles with a larger rolling resistance coefficient formed the looser filter cake. The reason for this was that the larger the particle rolling resistance coefficient, the greater the viscosity and the lower the sliding effect of the particles, leading to the more obvious phenomenon of "dendritic" deposition, which is consistent with a previous study [23].

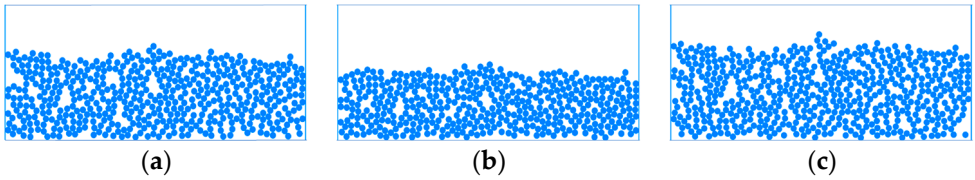


Figure 2. Comparison of deposition morphologies under different particle densities and rolling resistance coefficients (only layers 7, 8 and 9 are shown). (**a**) ρ = 1000, α = 0.2; (**b**) ρ = 2500, α = 0.2; (**c**) ρ = 1000, α = 0.5.

3.2. Effect of Particle Density on Filter Cake Properties

Figure 3 shows the calculated layered porosity and filtration resistance of the filter cake when the particle rolling resistance coefficient is 0.2 and the densities are 1000 and 2500 kg/m^3. With the increase in the particle deposition height, the layered porosity of the filter cake gradually increased from 0.3, while the layered filtration resistance decreased from 113 Pa. The corresponding filter cake deposition morphology (layers 1–7) was more compact when the particle density was 2500 kg/m^3 compared to when it was 1000 kg/m^3. The main reason for this was that the "bridging" phenomenon between particles was more obvious in the case of a higher particle density (referring to Figure 2a,b), and the number of particles in layers 1–7 of the filter cake was higher, resulting in a smaller filter cake porosity and a greater filtration resistance. Because the particles were densely distributed at the bottom, the eighth layer had fewer particles, which resulted in a higher porosity of the filter cake and a lower filtration resistance.

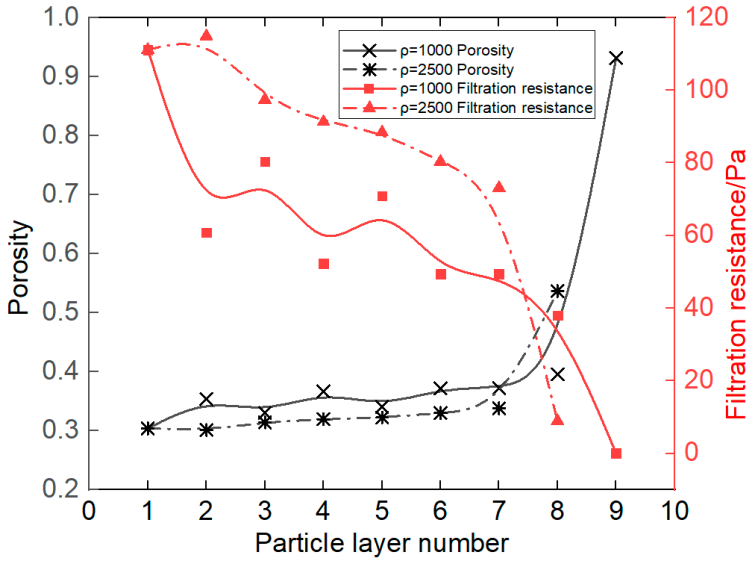


Figure 3. The effect of density on the filter cake porosity and the filtration resistance.

The effect of particle density on the average porosity and the total filtration resistance of the filter cake under different rolling resistance coefficients was further compared. Shown in Figure 4 are the average porosity and the total filtration resistance in cases of rolling resistance coefficients α of 0.2 and 0.5. As the particle density increased, the average porosity of the filter cake decreased and the total filtration resistance increased. Particles with a higher rolling resistance coefficient had a smaller total filtration resistance, and the difference between the total filtration resistances in these cases increased with the increase in particle density. For example, when the particle density was 500 kg/m^3 and the rolling resistance coefficient was 0.5, the total filtration resistance of the filter cake was 324 Pa, which was 84 Pa lower than the rolling resistance coefficient of 0.2. When the density was 3000 kg/m^3, the total filtration resistance of the filter cake under the condition of a rolling resistance coefficient of 0.5 was 183 Pa lower than that under the condition of a rolling resistance coefficient of 0.2. It was shown that increasing the density would lead to an increase in the compressibility of the particle layer, a decrease in the average porosity of the filter cake and an increase in the total filtration resistance.

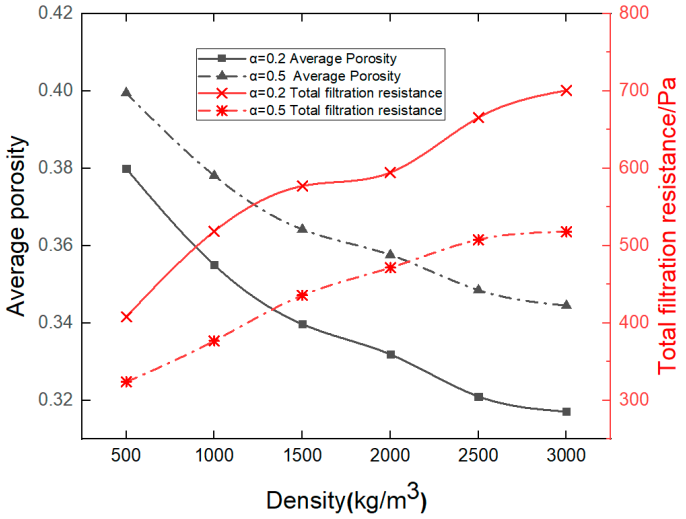


Figure 4. Effect of density on the average porosity and the total filtration resistance of the filter cake.

3.3. Influence of Particle Viscosity on Filter Cake Properties

The effect of the particle viscosity (characterized by the rolling resistance coefficient) on the filter cake porosity and the filtration resistance was further analyzed (Figure 5). When comparing the cases of rolling resistance coefficients α of 0.2 and 0.5 under a density of 1000 kg/m^3, it was found that the larger the rolling resistance coefficient, the larger the layered porosity of the filter cake and the smaller the filtration resistance. The variation trend of the layered filtration resistance of these cases was similar, but the values were very different. For example, in the first layer, when the rolling resistance coefficient α was 0.2, the filtration resistance was 115 Pa; when the rolling resistance coefficient α was 0.5, the filtration resistance was 67 Pa. It was found that, as the rolling resistance coefficient increased, the compressibility of the filter cake became lower, and the filtration resistance of the filter cake significantly decreased.

The average porosity and the total filtration resistance of the filter cake corresponding to the rolling resistance coefficients (0.1~1.0) are shown in Figure 6. In cases where the densities were 1000 kg/m^3 and 2500 kg/m^3, the average porosity of the filter cake increased with the increase in the rolling resistance coefficient; the total filtration resistance decreased as the rolling resistance coefficient increased; and the rate of decrease decreased with the increase in the rolling resistance coefficient. For example, when the density was 2500 kg/m^3 and the rolling resistance coefficient (α) was 0.7, the total filtration resistance was 403 Pa, which is 319 Pa lower than when the rolling resistance coefficient (α) was 0.1. This indicates that the more viscous the particle (the larger the coefficient of rolling resistance), the

lower the compressibility of the filter cake, and the filter cake showed a looser structure, resulting in an increase in the average porosity of the filter cake and a decrease in the total filtration resistance.

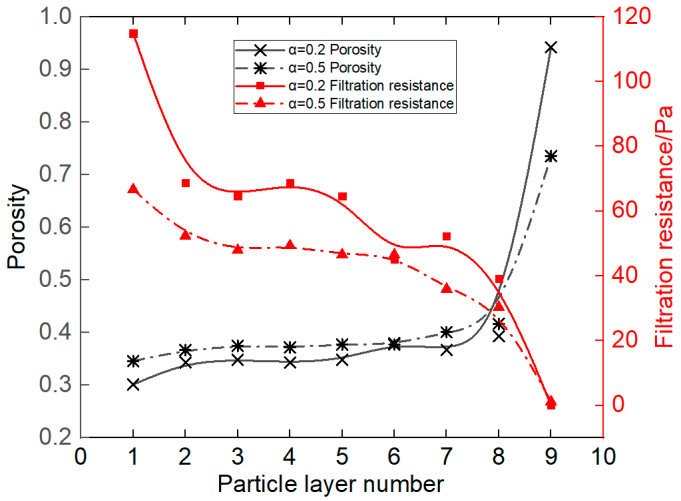


Figure 5. Effect of rolling resistance coefficient on average porosity and total filtration resistance of filter cake.

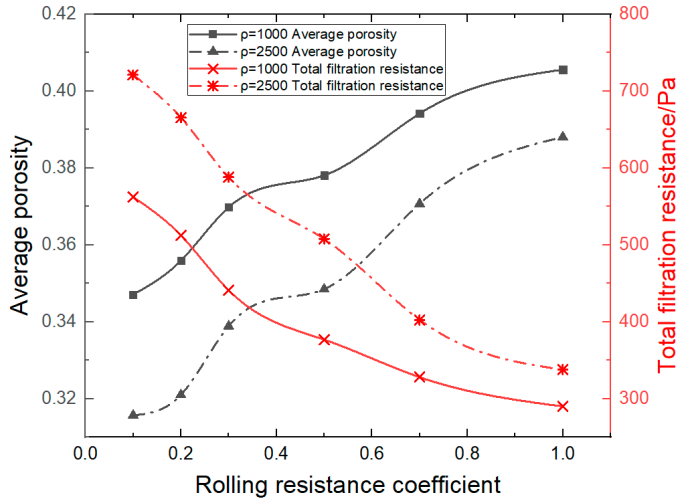


Figure 6. Effect of rolling resistance coefficient on average porosity and total filtration resistance of filter cake.

The variation found here indicates that the increase in particle viscosity led to a decrease in filtration resistance, which is consistent with the results in the literature [15,25–27]. It was reported that hygroscopic particles had a more significant effect on the viscosity, and the "dendritic" structure that formed was more obvious.

3.4. Influence of Air Humidity on Filter Cake Characteristics

An increase in the actual air humidity will increase the density and viscosity of particles at the same time, and these have opposite effects on the particle deposition characteristics (filtration resistance and porosity). Therefore, the final deposition characteristics need further discussion. Here, three different types of particles, DM828 (Starch), PVA1788 (Polyvinyl Alcohol) and Polyacrylamide (Polyacrylic acid), were selected for comparison. The experimental data of the equilibrium moisture regain R and the relative humidity RH of these three particles can be found in the literature [40]. The relationship between R and

RH was obtained by fitting the data points (Table 2), and the corresponding density of the particle could be obtained by the equilibrium moisture regain *R*.

Table 2. Relationship between the equilibrium moisture regain and relative humidity of particles.

Particle Name	PVA1788	Polyacrylamide	DM828
Fitting formula	$R = 0.1101RH - 0.4034$	$R = 0.6595e^{0.0501RH}$	$R = 0.2084RH - 0.1376$
Fitting degree R^2	0.9081	0.9917	0.9918

Figure 7 displays the relationship between the relative humidity, the average porosity $\bar{\varepsilon}$ and the total filtration resistance ΔP_t of the filter cakes with three different characteristics. It was found that with the increase in the relative humidity, the average porosity $\bar{\varepsilon}$ of Polyacrylamide and PVA1788 particles increased and the total filtration resistance gradually decreased, and the total filtration resistance ΔP_t of the filter cake decreased from 684 to 578 Pa and 692 Pa to 529 Pa, respectively.

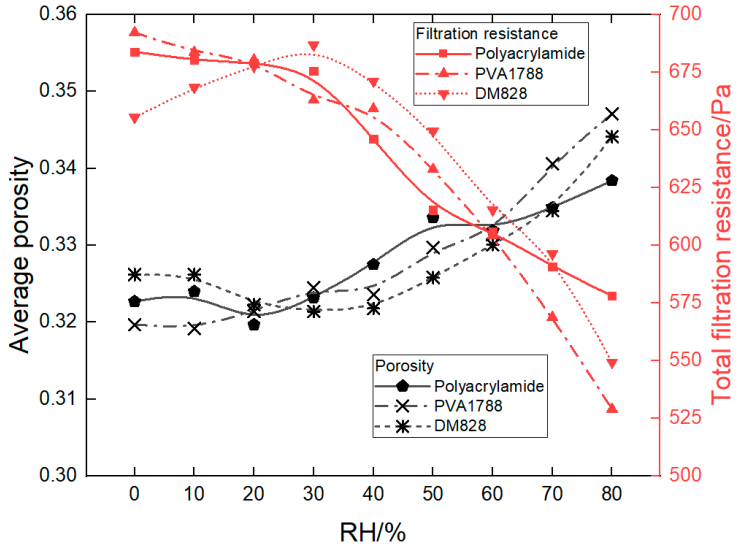


Figure 7. The effect of the relative humidity on the average porosity and the total filtration resistance of the three filter cakes.

In contrast, the average porosity $\bar{\varepsilon}$ of DM828 particles first decreased and then increased with the increase in relative humidity, and the total filtration resistance first increased and then decreased. In a relative humidity range from 0% to 30%, the total filtration resistance increased from 655 Pa to a maximum value of 687 Pa. In a relative humidity range from 30% to 80%, the total filtration resistance ΔP_t reduced to 549 Pa. This change was consistent with the variation in the deposition morphology of the filter cake, which first densified and then loosened with the increase in the relative humidity (Figure 8).

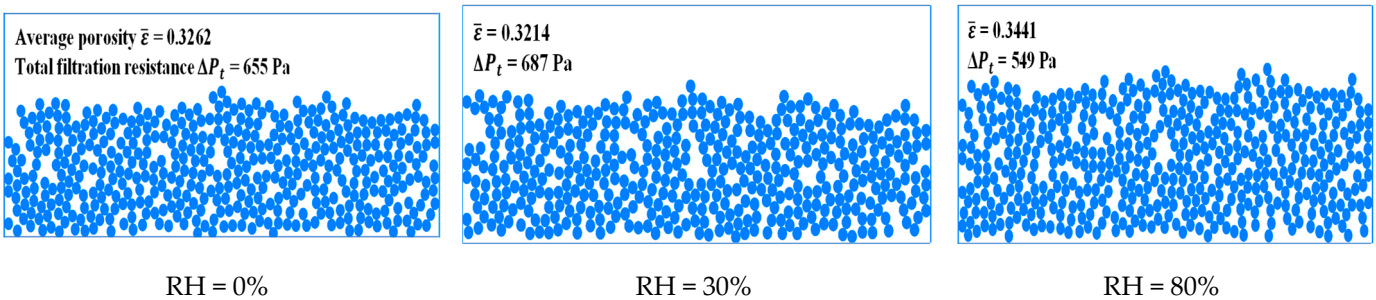


Figure 8. Three particle deposition patterns with different humidities (layers 7, 8 and 9).

It can be stated that since the increase in air humidity increased the density and viscosity of particles at the same time, the filtration resistance increased with the increase in density and decreased with the increase in viscosity. The total filtration resistance of Polyacrylamide and PVA1788 particles showed a monotonically decreasing trend with the increase in relative humidity, indicating that the particle viscosity was always the main influencing factor. The effect of air humidity on Polyacrylamide and PVA1788 particles was mainly reflected in the viscosity, while the effect on the density was relatively weak.

However, the influence of air humidity on the cake porosity and filtration resistance of DM828 particles had an inflection point. In a relative humidity range from 0% to 30%, the average porosity of the filter cake decreased and the total filtration resistance increased. In this range, the effect of the relative humidity on the filter cake was a minor factor, while the effect of the density was more significant. In the range of 30%–80%, the effect of air humidity on particle viscosity was greater than the effect on density. This phenomenon tells us that, when analyzing the particle filtration performance under humid conditions, a single factor, which changes with environment humidity, should not be considered but rather the actual changes of multiple factors.

Therefore, three kinds of variations can be determined based on our findings and the literature: as the humidity increased, (1) the filtration resistance first increased and then decreased (the porosity is inversely proportional to the filtration resistance); (2) the filtration resistance decreased; and (3) the filtration resistance increased.

Regarding the first type, such as DM828 studied here and the particle in reference [28], the particles were hygroscopic, and their moisture absorption was balanced (hygroscopic degree was high). When the relative air humidity was low, it had a slight effect on particle viscosity, leading to an obvious bridging phenomenon and, therefore, higher filtration resistance. When the relative humidity was high, it had an obvious effect on viscosity and led to lower resistance.

For the particles that were hydrophobic and not able to easily achieve a moisture absorption balance (such as the situation in reference [27], where the hygroscopic degree was low), as well as in the situation where humidity was added in the airflow just before the filtration and the particles did not have enough time to absorb the humid moisture [15,25–27], the adhesion between particles increased with the increase in humidity. In a certain humidity range (RH $\leq$ 80%), these particles readily formed a "dendritic" structure and belonged to the second variation type. Moreover, some particles whose viscosity was influenced more obviously than density by the humidity (Polyacrylamide and PVA1788 particles studied here) belonged to this type.

For the third type, such as the particles in reference [22,24], these particles were non-hygroscopic and their density and viscosity were slightly influenced by humidity. It was believed that, even with a low humidity, due to the capillary condensation of water, a dense particle cake was formed, resulting in an increase in resistance. Water adsorption on the particle surface (with a relative humidity value below 70%) and liquid bridges between particles formed by condensation changed the internal forces of the particles.

4. Conclusions

The PFC program was used to simulate the filtration of particles in a humid environment and realized the visualization of the particle deposition process. The influence of particle moisture on filter cake characteristics could provide a reference for filtration under different humidities and optimize the filtration system. When the particle density was greater or the rolling resistance coefficient was smaller, the "bridging" phenomenon among the particles was mainly exhibited, and the deposition morphology of the filter cake was more compact. On the contrary, the "dendritic" structure among the particles was more obvious, and the deposition morphology was looser.

The increase in air humidity increased the density and surface viscosity of the particles at the same time. The average porosity of the filter cake formed by the particles decreased with the increase in the density and increased with the increase in the rolling resistance co-

efficient. The total filtration resistance increased with the increase in density and decreased with the increase in surface viscosity.

The density and the viscosity of the particles varied in different degrees with humidity, which led to different trends in the properties of the filter cakes formed by the different particles with varying humidities. For DM828 particles, from the aspects of filtration resistance and porosity, when the relative humidity was less than 30%, the effect of humidity on particle density was greater than its effect on viscosity. When the relative humidity was between 30% and 80%, the effect of humidity on viscosity was dominant; the porosity of the filter cake first decreased and then increased with the increase in humidity, while the total filtration resistance first increased and then decreased. For the PVA1788 and Polyacrylamide particles, the effect of humidity on the viscosity was greater than its effect on the density. The porosity of the formed filter cake and the total filtration resistance varied monotonously.

According to the analysis and by combining the results with existing reports, three kinds of variations were found and could be divided according to the influence of humidity on filtration performance as follows: first, as the humidity increases, the filtration resistance first increases and then decreases; second, the filtration resistance decreases; and third, the filtration resistance increases. The hygroscopic degree should also be considered with the influence of humidity on the particle filtration performance.

Author Contributions: Conceptualization, J.L., D.S., Y.D., Q.W. and D.W.; software, D.S. and Y.D.; validation, J.L. and D.S.; data curation, D.S.; writing—original draft preparation, D.S.; writing—review and editing, D.S., J.L., Y.D., Q.W., S.H., H.H. and D.W.; supervision, J.L.; funding acquisition, J.L. and D.W. All authors have read and agreed to the published version of the manuscript.

Funding: This work was supported by the Natural Science Foundation of China (52064037, 51704166) and the Natural Science Foundation of Jiangxi Province (20202BAB204030).

Institutional Review Board Statement: Not applicable.

Informed Consent Statement: Not applicable.

Data Availability Statement: Not applicable.

Conflicts of Interest: The authors declare no conflict of interest. The funders had no role in the design of the study; in the collection, analyses, or interpretation of data; in the writing of the manuscript; or in the decision to publish the results.

References

1. Pu, H.; Luo, K.; Wang, P.; Wang, S.; Kang, S. Spatial variation of air quality index and urban driving factors linkages: Evidence from Chinese cities. *Environ. Sci. Pollut. Res.* **2017**, *24*, 4457–4468. [CrossRef] [PubMed]
2. Li, J.; Wu, Q.; Huang, Y.; Sun, Z.; Li, J.; Wu, D. Particulate matters filtration by a filter medium with pin holes: Modeling and experimental verification. *Process Saf. Environ. Prot.* **2022**, *158*, 282–290. [CrossRef]
3. Dentoni, V.; Grosso, B.; Pinna, F.; Lai, A.; Bouarour, O. Emission of Fine Dust from Open Storage of Industrial Materials Exposed to Wind Erosion. *Atmosphere* **2022**, *13*, 320. [CrossRef]
4. Adamkiewicz, Ł.; Maciejewska, K.; Rabczenko, D.; Drzeniecka-Osiadacz, A. Ambient Particulate Air Pollution and Daily Hospital Admissions in 31 Cities in Poland. *Atmosphere* **2022**, *13*, 345. [CrossRef]
5. Li, T.; Guo, Y.; Liu, Y.; Wang, J.; Wang, Q.; Sun, Z.; He, M.Z.; Shi, X. Estimating mortality burden attributable to short-term PM2.5 exposure: A national observational study in China. *Environ. Int.* **2019**, *125*, 245–251. [CrossRef] [PubMed]
6. Zanobetti, A.; Schwartz, J.; Dockery, D.W. Airborne particles are a risk factor for hospital admissions for heart and lung disease. *Environ. Health Perspect.* **2000**, *108*, 1071–1077. [CrossRef]
7. Dominici, F.; Peng, R.D.; Bell, M.L.; Pham, L.; Mcdermott, A.; Zeger, S.L.; Samet, J.M. Fine particulate air pollution and hospital admission for cardiovascular and respiratory diseases. *JAMA* **2006**, *295*, 1127–1134. [CrossRef]
8. Mazzeo, A.; Zhong, J.; Hood, C.; Smith, S.; Stocker, J.; Cai, X.; Bloss, W.J. Modelling the Impact of National vs. Local Emission Reduction on $PM_{2.5}$ in the West Midlands, UK Using WRF-CMAQ. *Atmosphere* **2022**, *13*, 377. [CrossRef]
9. Zaib, S.; Lu, J.; Bilal, M. Spatio-Temporal Characteristics of Air Quality Index (AQI) over Northwest China. *Atmosphere* **2022**, *13*, 375. [CrossRef]
10. Chen, S.; Wang, Q.; Chen, D.-R. Effect of pleat shape on reverse pulsed-jet cleaning of filter cartridges. *Powder Technol.* **2017**, *305*, 1–11. [CrossRef]

11. Wang, J.; Ponting, M.; Zhang, C.; Olah, A.; Baer, E. Fuel filtration properties and mechanism of a novel fibrous filter produced by a melt-process. *J. Membr. Sci.* **2017**, *526*, 229–241. [CrossRef]
12. Arunangshu, M.; Harshad, S.B. Emission of fine particles and ageing behavior of PTFE finished filter media during industrial pollution control. *Environ. Pollut.* **2015**, *4*, 58–68.
13. Li, J.; Wang, A.; Fan, B.; Kuang, Q.; Li, J.; Wu, D. On the fractional dust emission features of the dust collector during the pulse-jet cleaning affected stage. *J. Saf. Environ.* **2018**, *18*, 315–319.
14. Li, J.; Wang, P.; Wu, D.; Chen, D.-R. Numerical study of opposing pulsed-jet cleaning for pleated filter cartridges. *Sep. Purif. Technol.* **2019**, *234*, 116086. [CrossRef]
15. Li, J.; Zhou, F.; Li, S. Experimental study on the dust filtration performance with participation of water mist. *Process Saf. Environ. Prot.* **2017**, *109*, 357–364. [CrossRef]
16. Zhou, F.; Li, J.; Li, S.; Wang, F. Experimental investigation and application of dry-type filtering dust collection technology in fully mechanized excavation face. *J. China Coal Soc.* **2017**, *42*, 639–645.
17. Wang, G. *The Study of Behavior of ePTFE Membrane Filter in Air-Filtration Process*; Beijing University of Chemical Technology: Beijing, China, 2004.
18. Qing, T.; Shao, T.; Wen, S. Effects of relative humidity on surface adhesion. *Tribology* **2006**, *26*, 295–299.
19. Xue, Z.; Qian, F.; Zhu, J. Numerical simulation of deposition characteristics for high moisture viscous particles on the surface of polytetrafluoroethylene microporous membrane filtration materials. *Chin. J. Process Eng.* **2020**, *20*, 521–530.
20. Zhan, F. *Modeling and Validation of Dust Particle Deposition on Fin-and-Tube Heat Exchangers*; Shanghai Jiao Tong University: Shanghai, China, 2018.
21. Gupta, A.; Novick, V.J.; Biswas, P.; Monson, P.R. Effect of humidity and particle hygroscopicity on the mass loading capacity of high efficiency particulate air (HEPA) filters. *Aerosol Sci. Technol.* **1993**, *19*, 94–107. [CrossRef]
22. Ribeyre, Q.; Charvet, A.; Vallières, C.; Thomas, D. Impact of relative humidity on a nanostructured filter cake—Experimental and modelling approaches. *Chem. Eng. Sci.* **2017**, *161*, 109–116. [CrossRef]
23. Li, J.; Li, X.; Wu, D.; Wu, Q.; Li, J. Dynamic simulation for depositive regularity of cohesive particles on surface of filter media. *J. Saf. Environ.* **2019**, *19*, 978–984.
24. Boudhan, R.; Joubert, A.; Durécu, S.; Gueraoui, K.; Le Coq, L. Influence of air humidity on particle filtration performance of a pulse-jet bag filter. *J. Aerosol Sci.* **2019**, *130*, 1–9. [CrossRef]
25. Joubert, A.; Laborde, J.C.; Bouilloux, L.; Callé-Chazelet, S.; Thomas, D. Influence of Humidity on Clogging of Flat and Pleated HEPA Filters. *Aerosol Sci. Technol.* **2010**, *44*, 1065–1076. [CrossRef]
26. Joubert, A.; Laborde, J.; Bouilloux, L.; Chazelet, S.; Thomas, D. Modelling the pressure drop across HEPA filters during cake filtration in the presence of humidity. *Chem. Eng. J.* **2011**, *166*, 616–623. [CrossRef]
27. Yuan, X.; Chen, X.; Yang, Z.; Yang, F.; Yang, J.; Zhang, W. Effects of humidity on dust removal intensification of bag filters. *J. Chem. Eng. Chin. Univ.* **2019**, *33*, 965–971.
28. Li, J.; Li, S.; Zhou, F. Effect of moisture content in coal dust on filtration and cleaning performance of filters. *Physicochem. Probl. Miner. Process.* **2016**, *52*, 365–379.
29. Shi, C.; Zhang, Q.; Wang, S. *Particle Flow (PFC5.0) Numerical Simulation Technology and Application*; China Construction Industry Press: Beijing, China, 2018.
30. Ai, J.; Chen, J.; Rotter, J.M.; Ooi, J.Y. Assessment of rolling resistance models in discrete element simulations. *Powder Technol.* **2011**, *206*, 269–282. [CrossRef]
31. Chen, L.; Qian, F.; Ye, M.; Wei, M.; Han, Y.; Lu, J. Mathematical model of high-humidity dust peeling during pulse-jet cleaning. *J. China. Coal Soc.* **2019**, *2*, 683–690.
32. Xie, H. *Powder Mechanics and Engineering*; Chemical Industry Press: Beijing, China, 2003.
33. Payam, A.F.; Fathipour, M. A capillary force model for interactions between two spheres. *Particuology* **2011**, *9*, 381–386. [CrossRef]
34. Xiong, G.; Gao, Z.; Hong, C.; Qiu, B.; Li, S. Effect of the rolling friction coefficient on particles' deposition morphology on single fibre. *Comput. Geotech.* **2020**, *121*, 103450. [CrossRef]
35. Liu, X.; Wu, C.; Sun, G.; Chen, B. Correlation analysis of blast furnace slag fly ash mixture of the macro micro mechanics parameter. *J. Civ. Eng. Manag.* **2015**, *32*, 1–7.
36. Sun, Q.; Wang, G. Review on granular flow dynamics and its discrete element method. *Adv. Mech.* **2008**, *38*, 87–100.
37. Shen, Z.; Jiang, M.; Zhu, F.; Hu, H. Influence of the micro parameters of discrete element on the macro parameters of sands. *Northwestern Seismol. J.* **2011**, *33*, 160–165.
38. Zhou, B.; Wang, H.; Zhao, W.; Li, J.; Zhen, B. Analysis of relationship between particle mesoscopic and macroscopic mechanical parameters of cohesive materials. *Rock Soil Mech.* **2012**, *33*, 3171–3175.
39. Carman, P.C. Fundamental principles of industrial filtration (A critical review of present knowledge). *Trans. Inst. Chem. Eng.* **1938**, *16*, 168–188.
40. Wu, H.; Yao, Y.; Shen, Y. Moisture absorption and liberation regularities of textile sizes. *Text. Res. J.* **2016**, *37*, 72–77.